Cancer Cell
Article

Downregulation of p53-inducible microRNAs *192*, *194*, and *215* Impairs the p53/MDM2 Autoregulatory Loop in Multiple Myeloma Development

Flavia Pichiorri,[1,2,10,*] Sung-Suk Suh,[1,2,10] Alberto Rocci,[3] Luciana De Luca,[4] Cristian Taccioli,[1,5] Ramasamy Santhanam,[1] Wenchao Zhou,[6] Don M. Benson, Jr.,[7] Craig Hofmainster,[7] Hansjuerg Alder,[1] Michela Garofalo,[1] Gianpiero Di Leva,[1] Stefano Volinia,[1,8] Huey-Jen Lin,[6] Danilo Perrotti,[1] Michael Kuehl,[9] Rami I. Aqeilan,[1,2] Antonio Palumbo,[3] and Carlo M. Croce[1,*]

[1]Departments of Molecular Virology, Immunology and Human Genetics, Comprehensive Cancer Center, Ohio State University, Columbus, OH 43210, USA
[2]IMRIC-The Lautenberg Center for Immunology and Cancer Research, Hebrew University-Hadassah Medical School, Jerusalem, Israel 91120
[3]Division of Hematology, University of Turin, Turin, Italy 10149
[4]Molecular Oncology Unit, IRCCS, Referral Cancer Center of Basilicata-Crob, Rionero in Vulture (PZ), Italy 85028
[5]Cancer Institute, University College London, London WC1E, UK
[6]Medical Technology Division, School of Allied Medical Professions, Ohio State University, Columbus, OH 43210, USA
[7]Division of Hematology and Oncology, Department of Medicine, Comprehensive Cancer Center, Ohio State University, Columbus, OH 43210, USA
[8]Telethon Facility-Data Mining for Analysis of DNA Microarrays, Department of Morphology and Embryology, University of Ferrara, Ferrara 44100, Italy
[9]Genetics Branch, Center for Cancer Research, National Cancer Institute, Bethesda, MD 20889-5105, USA
[10]These authors contributed equally to this work
*Correspondence: flavia.pichiorri@osumc.edu (F.P.), carlo.croce@osumc.edu (C.M.C.)
DOI 10.1016/j.ccr.2010.09.005

SUMMARY

In multiple myeloma (MM), an incurable B cell neoplasm, mutation or deletion of p53 is rarely detected at diagnosis. Using small-molecule inhibitors of MDM2, we provide evidence that miR-*192*, *194*, and *215,* which are downregulated in a subset of newly diagnosed MMs, can be transcriptionally activated by p53 and then modulate MDM2 expression. Furthermore, ectopic re-expression of these miRNAs in MM cells increases the therapeutic action of MDM2 inhibitors in vitro and in vivo by enhancing their p53-activating effects. In addition, miR-*192* and *215* target the IGF pathway, preventing enhanced migration of plasma cells into bone marrow. The results suggest that these miRNAs are positive regulators of p53 and that their downregulation plays a key role in MM development.

INTRODUCTION

The tumor suppressor p53 is frequently inactivated by mutations or deletions in cancer. p53 acts as a potent transcription factor and can be activated in response to diverse stresses, leading to induction of cell-cycle arrest, apoptosis, or senescence (Junttila and Evan, 2009; Xue et al., 2007). Although regulation of the p53 pathway is not fully understood at the molecular level, it has been well established that activated p53 suppresses cancer progression, underlining why cancer cells have developed multiple mechanisms to disable p53 function (Danovi et al., 2004; Ventura et al., 2007). In human tumors that retain wild-type (WT) p53 (Junttila and Evan, 2009; Lane, 2001) p53 can be antagonized by murine double minute 2 (MDM2), a negative

Significance

Therapeutic activation of p53 may be particularly appropriate for treatment of the ~50% of hematopoietic malignancies with intact *TP53*. We describe a signaling pathway in which miR-*192*, *194*, and *215* are regulators of the MDM2/p53 auto regulatory loop, controlling the balance between p53 and MDM2 expression. Hypermethylation of the miR-*194-2-192* cluster promoter in MM cell lines suggests that epigenetic downregulation of these miRNAs, which leads to increased MDM2 mRNA and protein expression, decreases the ability of p53 to downmodulate MDM2 expression, thus tipping the regulatory loop in favor of MDM2. Exploring these miRNAs as enhancers in the pharmacological activation of the p53 pathway in MM cells might open avenues for miRNA-targeted therapies and MM treatment.

regulator of p53 that is also overpriced in many human tumors, offering a therapeutic strategy (Dickens et al., 2009; Brown et al., 2009). It has been reported that inhibiting MDM2 expression can reactivate p53 in cancer cells, leading to their demise (Dickens et al., 2009; Saha and Chang, 2010).

TP53 mutation is rarely detected at diagnosis in many hematological cancers such as multiple myeloma (MM), acute myeloid leukemia, chronic lymphocytic leukemia, and Hodgkin's disease (HD). Thus, numerous reports have shown that therapeutic induction of p53 might be particularly suitable for the treatment of hematological malignancies (Saha and Chang, 2010). Among them, multiple myeloma (MM) is a currently incurable plasma cell proliferative disorder that results in considerable morbidity and mortality (Kuehl and Bergsagel, 2002; Fonseca et al., 2009). MM develops from a benign condition called monoclonal gammopathy of undetermined significance (MGUS) (Weiss et al., 2009). Individuals with MGUS often remain stable for years and do not require treatment. However, for unknown reasons, this benign condition can evolve into MM at a rate of ~1% per year, with some MMs developing after many years (Kuehl and Bergsagel, 2002; Fonseca et al., 2009).

In MGUS and in the majority of newly diagnosed MM cases *TP53* is WT (Kuehl and Bergsagel, 2002; Chng et al., 2007) and the protein is rarely detectable (Stuhmer and Bargou, 2006). Interestingly, in MM cells, expression of p53 protein levels can be rescued by antagonizing MDM2. Several reports have focused on the p53-mediated apoptotic pathway, upon endogenous p53 protein re-expression by the small-molecule MDM2 antagonists (Nutlins) and target genes which may be involved in p53-dependent apoptosis in MM cells have been identified (Stuhmer and Bargou, 2006).

MicroRNAs are an abundant class of short, non-protein-coding RNAs that mediate the regulation of target genes post-transcriptionally and that have emerged as master regulators in diverse physiologic and pathologic processes (Bartel, 2004), and oncogenesis (Croce, 2008). Recently, microRNAs (miRNAs) have been reported to be directly transactivated by p53 (He et al., 2007). miRNAs have also been shown to target p53 and/or components of p53 regulatory pathways, thereby directly and/or indirectly affecting its activities (Park et al., 2009; Zhang et al., 2009). We previously published the global miRNA-expression profiles of MM and MGUS and contrasted these profiles with those of normal plasma cells (PCs) (Pichiorri et al., 2008). The findings defined a miRNA signature related to expression and regulation of proteins associated with malignant transformation of PCs, such as p53 (Pichiorri et al., 2008). We have now examined the regulation and functional roles of miRNAs in MM development using small-molecule inhibitors of MDM2.

RESULTS

Identification of p53-Regulated miRNAs in MM

To determine if miRNAs are regulated by p53 in MM cells, we performed custom microarray analysis with an expanded set of probes capable of assaying the expression of more than 500 human miRNAs. Two approaches to compare the effect of p53 level on miRNA expression were used. We first assessed a specific signature associated with the presence of WT *TP53* in MM cell lines as shown in Figure 1A and Table S1 available online. Six MM cell lines were used in the analyses: MM1s, NCI-H929, and KMS28BM which retain and express WT *TP53*; RPMI-8226, U266 with mutant *TP53*; and JJN3 that does not express *TP53* mRNA. Western blot analysis of these cells shows their p53 and MDM2 steady-state protein levels, respectively (Figure S1A). Genomic and cDNA sequence analyses confirmed the presence of WT *TP53* cells in association with higher *MDM2* mRNA expression (Figure S1B). Several differentially expressed miRNAs were identified (Table S1). Some of these miRNAs, such as those of miR-*34* family, have been found to be associated with p53 status in other human malignancies (Hermeking, 2010). In the second approach, we performed miRNA microarray analysis in MM1s cells treated with or without Nutlin-3a (10 μM), a small-molecule inhibitor of MDM2 (Figure 1B). In response to Nutlin-3a treatment, we identified expression of distinct miRNAs associated with p53 activation (Figure 1B; Table S2). Only two miRNAs were upregulated in both analyses: miR-*34a* and miR-*194* (Figures 1A and 1B; Tables S1 and S2). These results not only confirm upregulation of miR-*34*a as a function of wild-type (WT) p53 status (He et al., 2007) but also point to strong upregulation of miR-*194* by p53 (Tables S1 and S2; Figures 1A and 1B). The significant upregulation of miR-*192* and miR-*215* after p53 re-expression through Nutlin-3a treatment is especially interesting because they are located, together with miR-*194,* in two related microRNA clusters, the miR-*194-2-192* cluster at 11q13.1 and the miR-*215-194-1* cluster at 1q41.1 (Table S2), and have the same seed sequence. Genomic locations of these two clusters have been reported to be important for MM (Fonseca et al., 2009). miR-*194* also has the same mature sequence regardless its expression cluster and miRNAs of the same cluster are usually expressed together (Garofalo et al., 2009; Ventura et al., 2008).

p53 Induces the Expression of miR-*192, 194*, and *215*

To confirm the microarray data, we first tested by q-RT-PCR for the presence of miR-*34a*, miR-*194*, and its cluster associate, miR-*192* and *215,* in WT *TP53* compared with Mut *TP53* cells (Figure S1C). WT *TP53* cells retained higher expression of miR-*34a*, miR-*194*, and miR-*192* (Figure S1C), but did not show expression of miR-*215*, suggesting that the 11q13.1 miR-*194-2-192* cluster is associated with WT *TP53* status in MM cells. To determine the kinetics of p53 activation, we treated MM1s cells with 10 μM Nutlin-3a for different duration of time. p53 was barely detectable by immunoblotting at 6 hr but increased after 12, 18, and 24 hr of treatment and remain constant at 30–36 hr (Figure 1C). The induction of p53 was also associated with MDM2 accumulation, p21 expression, and c-MYC downregulation after 12 hr of treatment (Figure 1C). The expression of p21-encoding *CDKN1A*, a p53 target gene, was also assessed by RT-PCR (Figure 1D). By northern blot and qRT-PCR analysis, we also studied the kinetics of miRNA activation during p53 upmodulation in MM1s cells. The kinetics of miR-*34a*, miR-*194*, miR-*192*, and miR-*215* expression (Figure 1E) were directly correlated with p53 protein upregulation and p21 activation (Figures 1C and 1D), while for miR-*15* and miR-*29a/b* the dynamics of expression appeared more related to downregulation of their repressor c-MYC as expected (Chang et al., 2008; Figures S1D and S1E; Figure 1D), than to p53 activation. To confirm the responsiveness of these miRNAs to p53, cell lines

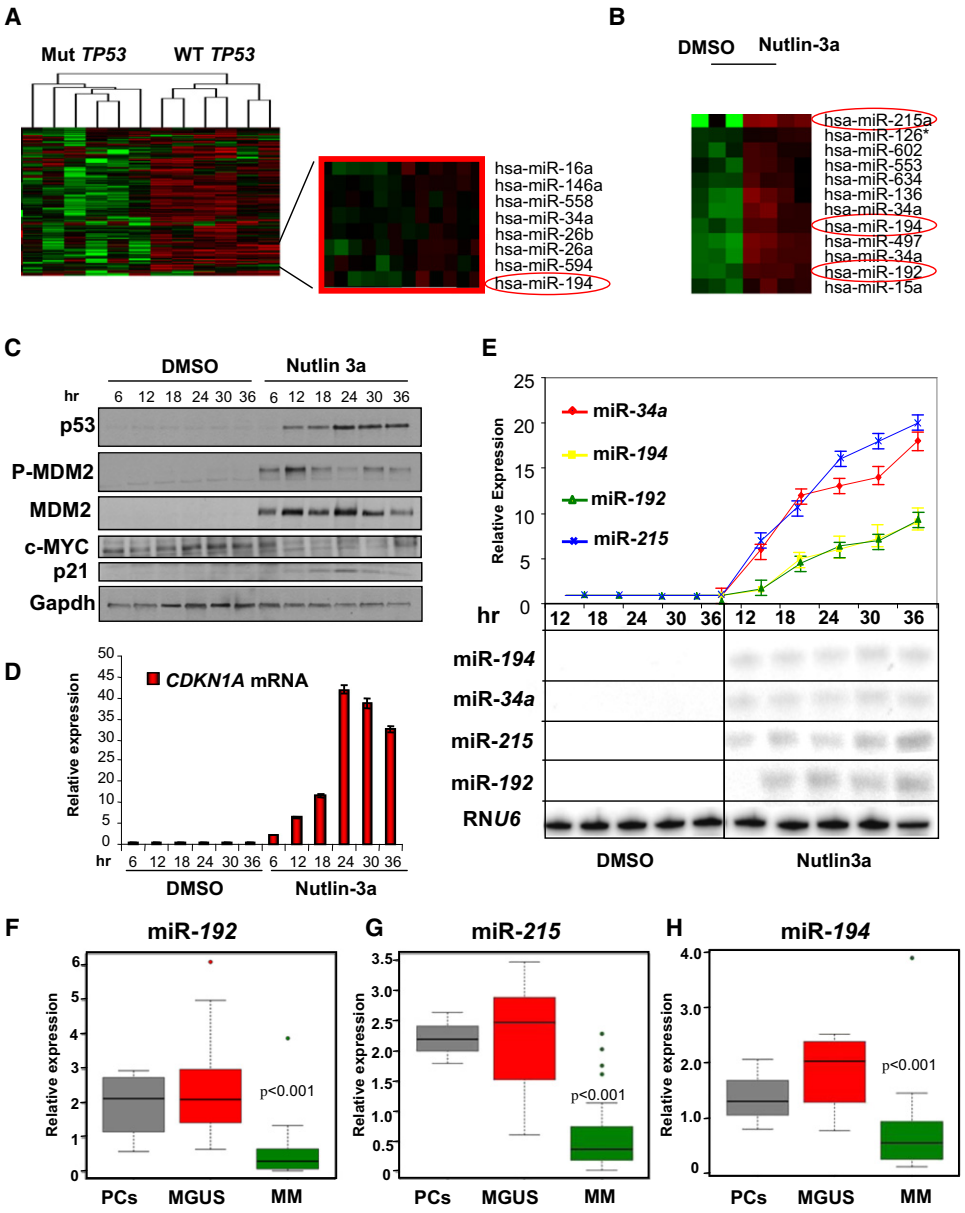

Figure 1. Identification of p53-Regulated miRNAs in MM Cells

(A) Overview of two-way (genes against samples) hierarchical cluster (Euclidean distance) of 6 MM cell lines in duplicate using the genes that vary the most between samples. As shown, the clustering is mainly determined by the presence of WT TP53 expression (NCI-H929, MM1s, and KMS28BM) or mutant/null TP53 (U266, RPMI-8226, JJN3) in the cell lines. In magnification are reported the miRNAs upregulated more than 3-fold in WT TP53 cell lines with $p < 0.001$. See also Figure S1 and Table S1.

(B) Overview of two-way of MM1s cells treated with 10 μM Nutlin-3a overnight (biological quadruplicate) and with DMSO (biological triplicate) using the genes that vary the most between samples. As shown, the clustering is mainly determined from the Nutlin-3a treatments and DMSO treatment. Color areas indicate relative expression of each gene with respect to the gene median expression (red above, green below the median value, and black, samples with signal intensity to background of 2 or less). See also Figure S1 and Table S2.

(C and D) Western blot analysis of p53, MDM2, phosphor(p)-MDM2, c-MYC, p21, and Gapdh (C) and time course of CDKN1A mRNA expression by RT-PCR in Nutlin-3a-treated (10 μM) MM1s cells (D). The PCR products were normalized to ACTIN expression. Values represent mean observed in four different studies ±SD.

(E) Kinetics of miR-194, miR-192, miR-215, and miR-34a in MM1s cells after Nutli-3a treatment, measured by qRT-PCR and northern blot analysis. Lines represent relative fold changes between DMSO and Nutlin-3a treatment ±SD. RNU44 (qRT-PCR) and RNU6B (northern blot) expression was used for normalization. See also Figure S1.

(F–H) miR-192, miR-215 and miR-194 relative expression in CD138+ PCs from healthy, MGUS, and MM samples (see Table S3) were determined by Taqman q-RT PCR assay. Each data sample was normalized to the endogenous reference RN*U44* and RN*U48* by use of the 2– ct method. The relative expression values were used to design box and whisker plots. Dots in the boxes indicate outlier points. Kruskal-Wallis analysis assessed that the three miRNAs were differentially expressed among MGUS samples versus MM PCs samples of the Bartlett test $p \leq 0.001$.

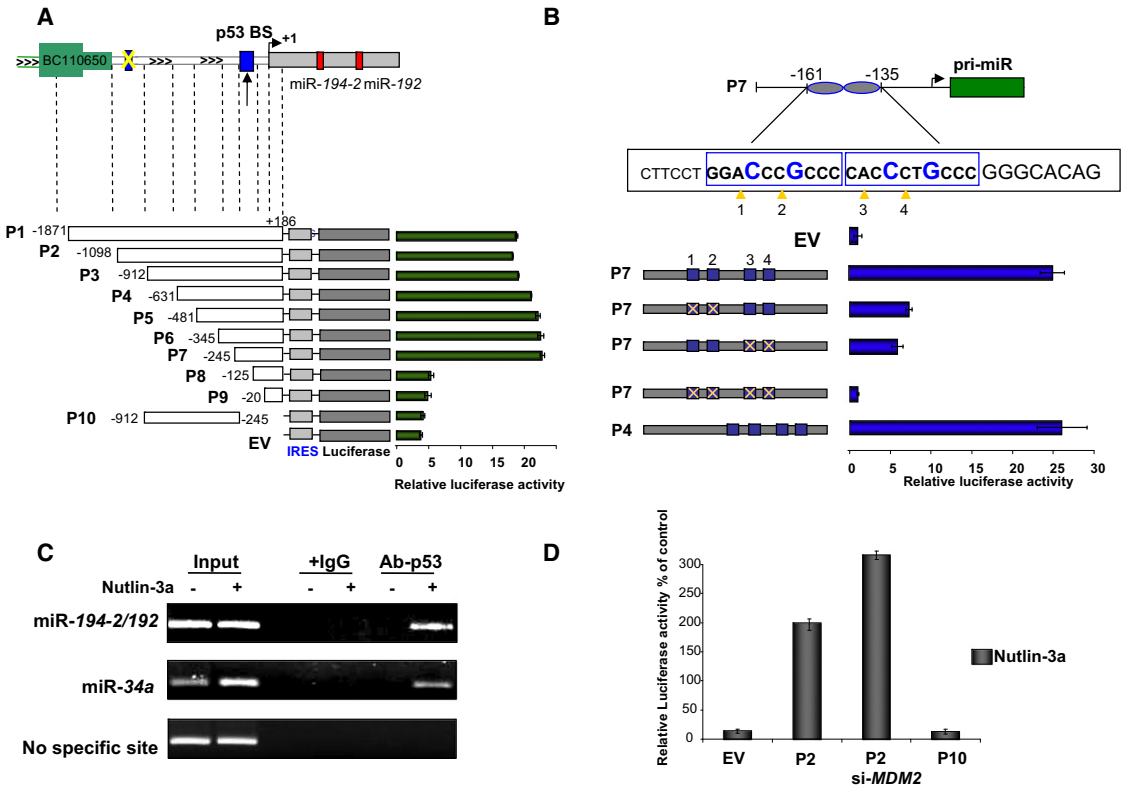

Figure 2. miR-*194-2-192* Cluster Is Induced Following p53 Activation

(A) Luciferase reporter activity of promoter constructs of miR-*192-194-2* cluster on chromosome 11q13.1 in MM1s cells after p53 transfection ±SD. The arrow above construct P1 indicates the position of the transcription start site +1. p53 binding sites (BD) are indicated (blue box).

(B) Relative luciferase activity of P7 reporter construct. The magnified sequence highlighted in blue shows the location of the El Deiry p53 consensus binding sites in P7 construct sequence. Deletions introduced into the P7 construct are shown in yellow (X) showing abolition of the promoter activity.

(C) Chip assay after 24 hr of p53 nongenotoxic activation, showing binding of p53 to the miR-*192-194-2* cluster promoter in vivo in MM1s cells.

(D) Luciferase activity of empty vector (EV), P2 and P10 reporter constructs after nongenotoxic activation of p53 and *MDM-2* mRNA silencing. Luciferase activities were normalized by Renilla luciferase activities. Values represent mean ± SD from three experiments.

See also Figure S2.

with varying *TP53* status were treated with Nutlin-3a or vehicle (DMSO), followed by qRT-PCR to monitor miRNA levels upon p53 activation (Figures S1F–S1K). Induction of miR-*34a*, miR-*192*, miR-*215*, and miR-*194* was detected only in the cell lines treated with Nutlin-3a and harboring WT *TP53* ($p < 0.001$, Figure S1). Next, we analyzed induction of these miRNAs, by Nutlin-3a in freshly isolated CD-138+ PCs (Figure S1L), from eight bone marrow aspirates of MM patients. Two samples (Pt-1 and Pt-2) exhibited *TP53* deletion by FISH analysis, while 6 (Pt-3 to Pt-8) retained *TP53* genes (Table S3). We detected induction of p53, miR-*34a*, *192, 194, 215* after 12 hr of Nutlin-3a treatment (Figures S1M–S1O) in *TP53* WT samples, in association with different levels of *CDKN1A* mRNA activation (Figure S1O). Furthermore, to determine if these miRNAs are relevant in MM pathogenesis, we analyzed the expression of miR-*194, 192*, and *215* in a panel of CD138+ PCs obtained from newly diagnosed MM patients (n = 33), MGUS (n = 14) patients and normal donors (n = 4) (Table S3) by qRT-PCR (Figures 1F–1H). Through Kruskal-Wallis analysis, we found that these clusters of miRNAs are consistently downregulated in MM samples ($p < 0.001$) compared with MGUS samples.

Identification of the p53 Core Element in the pri-miR-*192-194-2* Promoter at 11q13.1

To determine if p53 is directly involved in the transcriptional regulation of miR-*194-2-192* and miR-*215-194-1* clusters, we analyzed the cluster promoter regions. The upstream genomic region close to the transcription start site (TSS) (+1) (Hino et al., 2008) of pri-miR-*194-2-192* contains several highly conserved regions among human, mouse, rat, and dog sequences (from −162 to +21 with respect to the TSS). To identify the promoter region responsive to p53 re-expression, we constructed reporter plasmids carrying various genomic sequences around the TSS of the pri-miR-*194-2-192* cluster and subjected them to luciferase assay (Figure 2A). Bioinformatics search identified a previously reported high score p53 consensus site between −900/−912 bp (Sinha et al., 2008; Song et al., 2008); however, this site was not functional for p53 activation since luciferase reporter constructs excluding this region retained full activity (P3-P7) (Figure 2A). The region from −245 to +186 bp (P7) had promoter activity comparable to that of the longest regions in MM cells after forced expression of p53 (Figure 2A), but regions from −125 to +186 bp (P8)

and −912 to −245 bp (P10) did not. We identified a p53-responsive element between −245 and −125 bp (Figure 2B) because the construct excluding this region was not affected by p53 expression (Figure 2A). Since conserved regions in a given gene promoter are expected to contain regulatory elements, we focused on the highly conserved region controlling luciferase activity, the region between −161 and −135 bp. Luciferase assay using a construct mutated for each C and G contained in the two decamers of the hypothetical El-Deiry consensus sequence revealed that this unpredicted and previously unpublished region is critical for p53 transcriptional activation of the pri-miR-*194-2-192* cluster (Figure 2B). Indeed, we found that endogenous p53 directly interacts with the core element of the pri-miR-*194-2* promoter in MM1s cells, as demonstrated by CHIP assay after 12 hr of Nutlin-3a treatment (Figure 2C). As a positive control, we used the p53 consensus site on the miR-*34a* promoter, while a nonspecific sequence served as negative control (Figure 2C). Ectopic expression of p53 activated the promoter of both members of the pri-*miR-194-2-192* cluster in MM1s cells (Figure 2D). *MDM2* siRNA after p53 re-expression in MM1s cells led to higher relative luciferase activity and thus confirmed its dependence on p53 re-activation. Taken together, these data suggest that p53 is a key transcriptional activator of pri-miR-*194-2* through directly binding to the core promoter element (Figure 2D). We also attempted to identify the promoter and primary transcript of miR-*215-194-1* on chromosome 1q41.1, but could not identify the primary transcript initiation point by 3′ and 5′ RACE and PCR amplification of the putative transcribed sequences (ESTs); however, we confirmed the previously published consensus site for p53 by CHIP analysis (Figure S2).

miR-*192*, *194*, and *215* Affect p53-Dependent MM Cell Growth

To examine the relevance of p53-mediated regulation of miR-*192*, *194*, and *215* in MM, we first tested whether reintroduction of these miRNAs affected the biology of MM cells. Previous studies (Georges et al., 2008; Braun et al., 2008) showed that such reintroduction induced expression of p21 in different cancer cell lines which carried WT *TP53*, with a consistent G0/G1 arrest and p53 protein expression. The molecular mechanism of p53 re-expression remained elusive. To confirm this effect in our model, miR-*192*, miR-*194*, and miR-*215* were introduced into transfection in WT *TP53*-cell lines (MM1s, NCI-H929, and KMS28BM), as well as cells with mutated *TP53* (RPMI-8226), followed by detection of *TP53* and mRNAs of target genes *CDKN1A* and *MDM2*, by RT-PCR analysis (Figure S3). We found consistent re-expression of *CDKN1A* in *TP53* WT cells (Figure S3A) after transfection, but did not detect any increase in *TP53* mRNA (Figure S3B). Using MTS assay, we observed significant growth arrest in the cells transfected with *miR-192*, *215* and a less significant arrest with miR-*194* in MM cells carrying WT *TP53* (Figures 3A–3C), as compared with scrambled sequences. In contrast, we did not detect this effect in RPMI-8226 cells (Figure 3D) expressing mutant *TP53*. Next, we determined if p53-responsive miRNAs interfere with the clonogenic survival of MM cells. MM cells were lentivirus-transduced with miR-*192*, miR-*215*, miR-*194* and miR-*34a*, miR-*192*, and *215* in WT p53 cells suppressed colony formation to an extent comparable to miR-*34a*, which was used as an internal control. Of note, miR-*194* was less effective than miR-*215* and miR-*192*. These miRNAs did not suppress colony formation in RPMI-8226 (Figures 3E and 3F) or U266 cells (F.P., S.-S.S., C.M.C, unpublished data), while miR-*34a* did exhibit colony suppression in these mutant *TP53* cells, confirming its p53-independent apoptotic action (Hermeking, 2010).

To further explore the p53-dependent mechanism(s) of miR-*192*, *215*, and *194* interferences with cell growth and colony formation, we used flow cytometry to determine if their expression affects progression through the cell cycle. We noted that in the two WT *TP53* cell lines with high expression of *MDM2* mRNA, MM1s and NCI-H929 (Figure S1B), the p53-responsive miRNAs induced a consistent G0/G1 arrest. This effect was observed in ∼30% of scrambled-transfected cells versus ∼60% of the cells transfected with miR-*192* and *215* and ∼45% for miR-*194* (Figures 3G and 3H). By contrast in KMS-28BM cells, retaining WT *TP53* but expressing lower levels of *MDM2* mRNA (Figure S1B), we detected increases of sub-G_1 fractions (indicative of cell death) in cells transfected with miR-*192* (∼25% sub-G_1), *215* (30%), and *194* (12%) at 48 hr after transfection, compared with ∼3% in control cells transfected with the Scr sequence (Figure 3I). At 48 hr after transfection, we also detected increased caspase-3 activity (Figure 3J). The differential effect of the miRNAs on *TP53* WT cells carrying lower *MDM2* mRNA basal expression (Figure S1B) led us to analyze MDM2 levels after miRNA transfection (Figure S3C). *MDM2* mRNA, but not protein, was detected after MM cells transfection. Because MDM2 protein is rapidly autoubiquitinated and degraded through the proteasome pathway (Marine and Lozano, 2010); p53 induction is necessary for its detection in MM cells (Stuhmer and Bargou, 2006; Ooi et al., 2009). Only in one (Mut *TP53* RPMI-8226) of six MM cell lines analyzed was MDM2 protein detected without p53 activation (Figures S1A and S1G). We also noted that *MDM2* mRNA was downregulated after ectopic expression of these miRNAs, mostly in *WT TP53* cells, but to some extent also in Mut *TP53* cells (RPMI-8226) (Figure S3C). These data were confirmed at the protein level in RPMI-8226 cells where we observed ∼20% downregulation of MDM2 protein at 72 hr after miRNA transfection (Figure S3D). The results indicate that ectopic expression of miR-*192*, *215*, and *194* in WT *TP53* cells inhibits cell growth and enhances apoptosis, effects that could be related to MDM2 regulation in MM cells.

Human *MDM2* Is a Direct Target of miR-*192*, *194*, and *215*

The data thus far demonstrate that the biological functions of miR-*192, 215*, and *194* in MM cells is p53 dependent. After introduction of these miRNAs the *TP53* mRNA level did not change in MM cells but higher *CDKN1A* and lower *MDM2* mRNA levels were observed (Figure S3). Both genes, *MDM2* and *CDKN1A,* are direct targets of p53 but their expression in this case was not preceded by *TP53* transcription (Figure S3B). Thus, we hypothesized that miR-*192, 194* and *215* could target the expression of MDM2. To further examine the effects of these miRNAs on MDM2 protein expression in WT *TP53* MM cells, we analyzed the consequences of ectopic

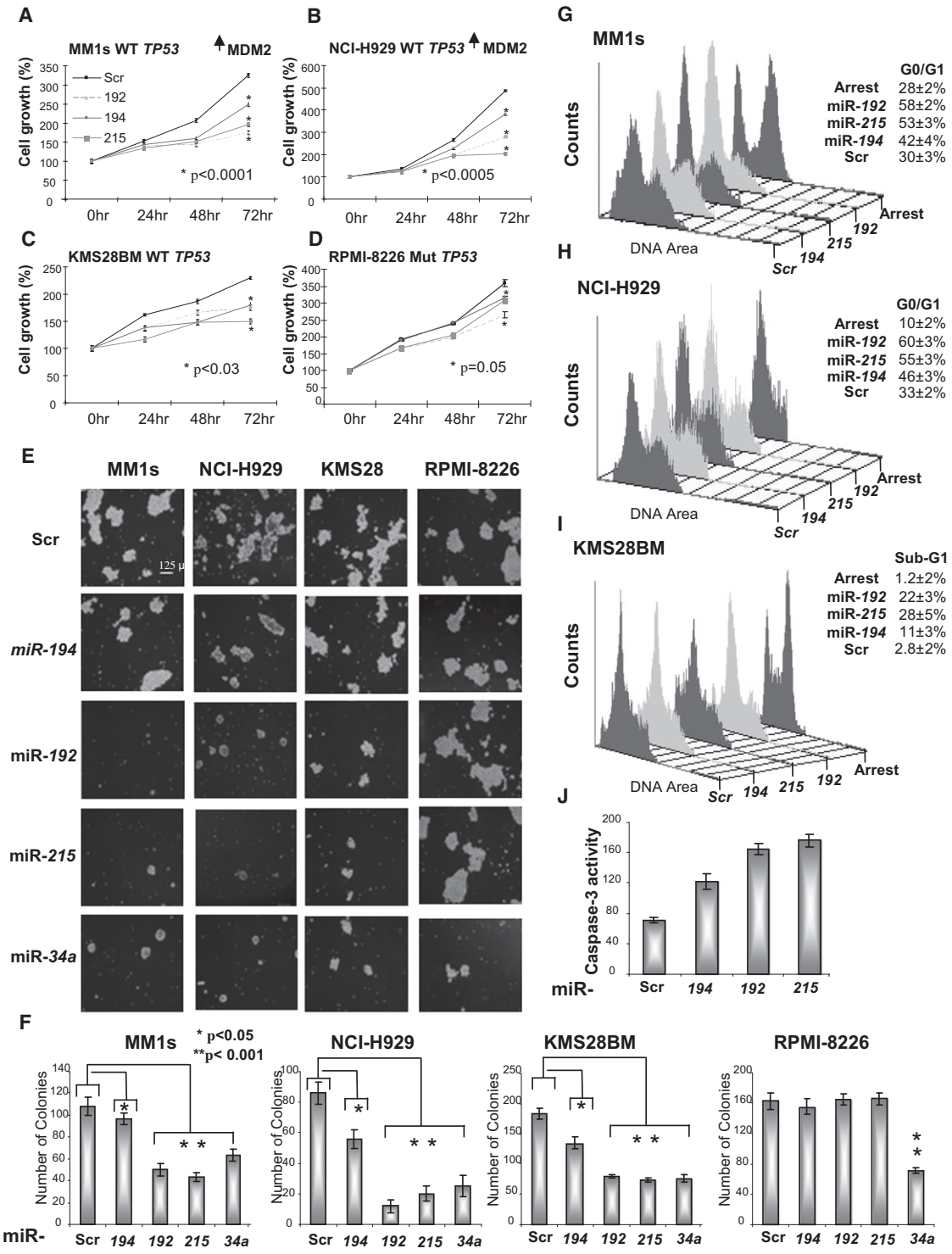

Figure 3. miR-*192-194-215* Induce Decrease of Proliferation and Cell-Cycle Arrest in WT *TP53* MM Cells

(A–D) MTS assay performed in MM1s (A), NCI-929 (B), KMS28BM (C), and RPMI-8226 (D) cell lines. Cells were transfected with miR-192, 194, 215, and scrambled sequence (Scr) and were harvested at 24, 48, and 72 hr after transfection. p values are indicated. See also Figure S3.

(E and F) Soft agar colony suppression assay in WT TP53 and mutant TP53 MM cell lines after miRNAs transduction by lentivectors.

(G–J) Flow cytometry analysis in MM1s (G), NCI-H929 (H), and KMS28BM (I) cells (miR-*192*, *194*, *215*, and Scr transfected) at 48 hr of transfection, after first being arrested and synchronized in G2/M phase by Nocodazole for 16 hr. Apoptosis in KMS28BM was evaluated by caspase-3 activity (J). All experiments were performed in triplicate ±SD.

expression of miR-*192,* miR-*194*, and miR-*215* at 72 hr after transfection and 12 hr of nongenotoxic activation of p53 by Nutlin-3a (10 μM). Increased expression of these miRs upon transfection was confirmed by qRT-PCR (Figure S4A), and the effects on p53, MDM2, and p21 levels were analyzed by western blot (Figure 4A). Overexpression of miR-*192, 194*, and miR-*215* significantly increased the level of p53 and p21 at 12 hr after Nutlin-3a treatment compared with Scr-transfected cells ($p < 0.001$), as shown by densitometric analysis in Figures 4B and 4C. Expression of MDM2 protein was dramatically decreased in both cell lines (Figures 4A–4C). Conversely, knockdown by 2′-O-me-anti-miR-*192-194* and *215* (pool) after 12 hr of Nutlin-3a treatment, as confirmed by qRT-PCR (Figure S4B) in *TP53* WT cell lines, increased the level of MDM2 protein ($p < 0.01$), while p21 and p53 protein levels were attenuated ($p < 0.01$) (Figure 4B), as confirmed by densitometry (Figure 4E). We also confirmed that *MDM2* mRNA levels were strongly reduced in the miR-*192*-, *194*-, and *215*-transfected cells at 6 and 12 hr of Nutlin-3a treatment in both cell lines (Figures 4C). These results indicate that miR-*192*, *194*, and *215* induce the degradation of *MDM2* mRNA, confirming that they regulate both, protein and RNA levels. We next tested whether *MDM2* is a direct target of these miRNAs by performing a bioinformatics search (Target Scan [Lewis et al., 2003]; Pictar Pictar [Krek et al., 2005]) but were unable to identify the 3′UTR of *MDM2* as a target. Because the 3′UTR of *MDM2* is not well conserved across species, we decided to use the RNA22 target prediction program (Miranda et al., 2006) which does not need validated targets for training, and neither requires nor relies on cross-species conservation. RNA22 predicted two miRNA-responsive elements (MREs) for miR-*192/215* and two MREs for miR-*194* in the 3′UTR of human *MDM2* (*HDM2*) (Figures 4D; Figures S4C–S4G). To verify that *HDM2* is a direct target of miR-*192,* miR-*194*, and miR-*215*, *HDM2* 3′UTR containing all MREs (~4K), was cloned into pGL3 basic construct downstream of the luciferase open reading frame (Figure 4D). This reporter construct was used to transfect MM1s cells which express the endogenous miRs following upmodulated p53 expression. Increased expression of these miRs upon transfection significantly diminished luciferase expression (Figure 4D). We subsequently screened the predicted MREs on the 3′UTR of *HDM2* mRNA, using luciferase assays with four different constructs carrying the MREs for miR-*192/215* and miR-*194* (Figures S4H–S4K). We observed that expression of each specific MRE reporter construct was specifically downregulated upon transfection of each individual miRNA. Conversely, when we performed luciferase assays using a plasmid harboring the binding sites inactivated by site-directed mutagenesis, we observed a consistent reduction in the inhibitory effects (Figures S4H–S4K). We also analyzed the expression of *MDM2* mRNA in a panel of CD138+ PCs obtained from MM patients, MGUS patients, and normal donors by RT-PCR (Figure 4E). Through Kruskal-Wallis analysis, we found that *MDM2* mRNA is significantly upregulated in MM samples ($p < 0.001$) compared with MGUS samples and normal PCs (Figure 4E). Using nonparametric test analysis, we found a significant inverse correlation between miR-*192* expression and *MDM2* mRNA in MM samples (Sperman $\rho = -0.698$, $p < 0.0001$, $n = 33$) (Figure 4F).

miR-*192*, *194*, and *215* Re-expression Enhances Sensitivity of WT *TP53* MM Cells to Nongenotoxic Activation of p53 In Vitro and In Vivo

To determine if re-expression of the miRNAs could enhance sensitivity of WT *TP53* MM cells to nongenotoxic activation of p53, we tested MI-219, a highly selective, orally active small-molecule inhibitor of the MDM2-p53 interaction (Shangary et al., 2008). We first examined whether MI-219 induces p53, MDM2, p21, and Puma upregulation in MM1s cells after miR-*192*, miR-*194*, and miR-*215* transfection. In cells with forced expression of miR-*192* and *215*, p53 became detectable even in untreated cells (Figures 5A and 5B) ($p < 0.05$), confirming previously published data in other cell lines (Georges et al., 2008; Braun et al., 2008). p53 re-expression and subsequent p21 and Puma upregulation was observed in these cells and in miR-*194*-transfected cells and is clearly visible following 24 hr of 2.5 μM MI-219 treatment (Figure 5A). In control cells (Scr), the treatment was ineffective (Figure 5A). Densitometric analysis of p53 and MDM2 protein levels was performed when cells were treated for 24 hr with 2.5, 5, and 10 μM MI-219 (Figure 5B). Confirming our previous data, we observed higher p53 accumulation (≥2-fold increase, $p < 0.001$) and dramatic MDM2 downregulation (≥3-fold decrease, $p < 0.001$) in miRNA-transfected cells (Figure 5B). These opposing changes in MDM2 and p53 expression levels correlated with higher activation of p53 downstream targets, p21 and Puma (Figure 5A). Furthermore, MI-219 induced higher caspase-3 activation in the presence of miR-*192*, miR-*194*, and miR-*215* ($p < 0.001$) (Figure 5C). Next, we examined whether activation of p53 by MI-219 leads to apoptosis in MM cells. Indeed, treatment with MI-219 induced apoptosis as revealed by Annexin V staining (Figure 5D). In cells transfected with a pool of miRNAs, MI-219 effectively ($p < 0.0002$) induced apoptosis at 2.5 μM (27% ± 3%) and 5 μM (32% ± 3%) while the scrambled control did not. This effect was less significant when using MI-219 at 10 μM (30% ± 5%), though it was enhanced when treatment was combined with miRNAs (55% ± 5%) (Figure 5D). Increased concentration of MI-219 did not increase the apoptotic rate of scrambled-transfected cells but caused nonspecific toxicity (data not shown). Because previous studies have shown that MI-219 achieved excellent oral availability, we investigated if, in mouse xenograft models, the combined action of miRNAs and oral MI-219 could suppress tumorigenicity of MM cells. Viable MM1s Gfp+/Luc+ cells (8×10^6) were injected subcutaneously into the right flank of 40 nude mice. At 3 weeks after injection a group of 32 mice with comparable tumor size were selected and randomly divided into four groups for four independent experiments, using eight mice for each combined treatment (Figure 5E). Specifically, we used the combination of oral treatment with 200 mg/kg MI-219 or vehicle control (VE) once a day for 14 days plus direct tumor injection of double-strand RNA scrambled sequence (Scr) or a pool of pre-miR-*192*, *194*, and *215* (miRs). Whereas the VE-Scr-treated tumors increased 2-fold in volume in 2 weeks (from 5390 ± 993 mm^3 to 13,500 ± 3200 mm^3 [$p < 0.0001$]), MI-219/Scr-treated tumors remained static in volume (5390 ± 993 mm^3 to 5400 ± 1200 mm^3) (Figure 5E). By contrast, mice treated with VE-miRs showed ~1.5-fold reduction in tumor size (from 5390 ± 993 mm^3 to

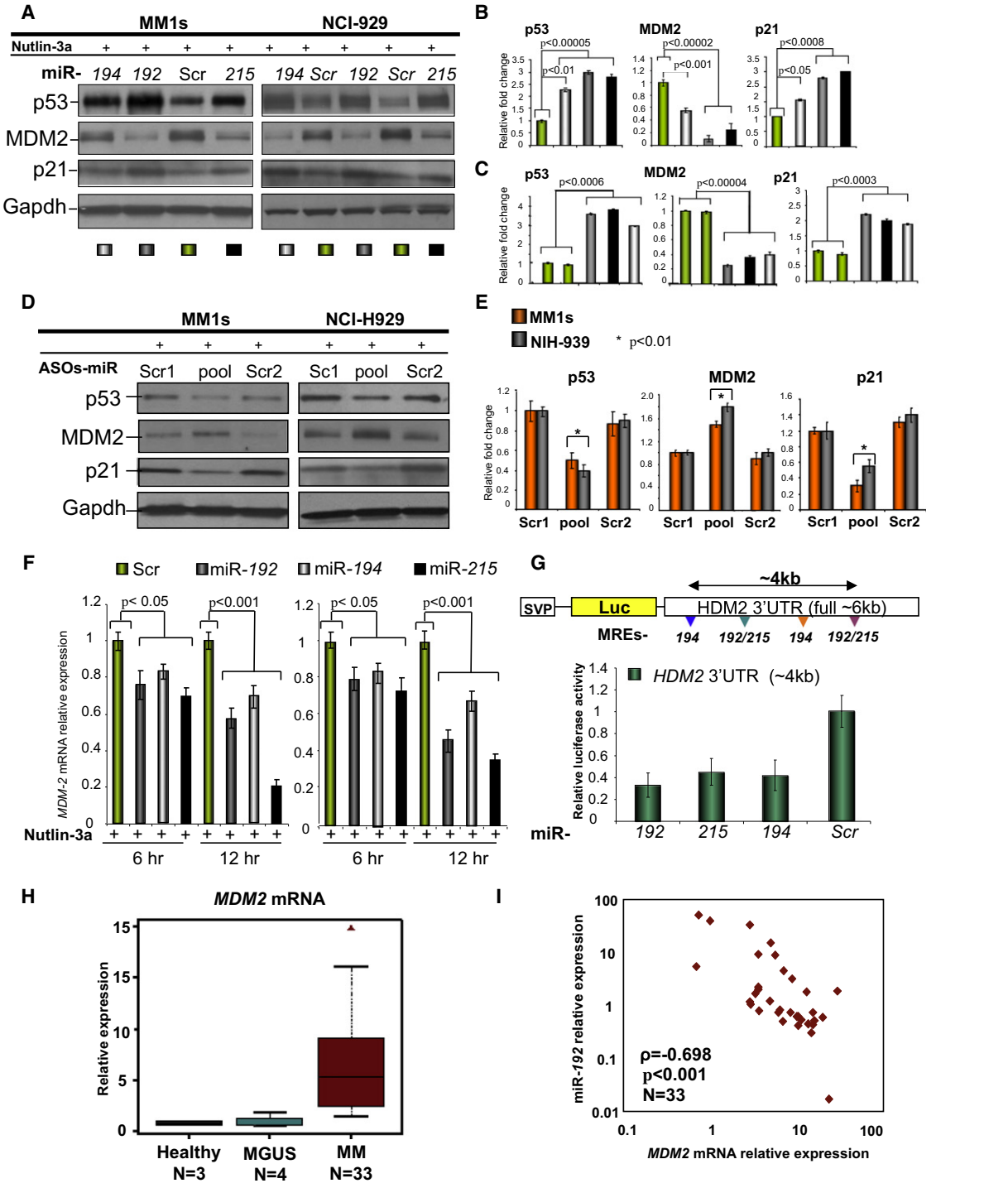

Figure 4. miRNA-192-194 and 215 Target MDM2 at the mRNA and Protein Levels in MM Cells

(A) MM1s and NCI-H929 cells (pre-miRNA-192, 194, 215, Scr sequence-transfected) were harvested at 72 hr after transfection and 12 hr Nutlin-3a treatment (10 μM). Whole-cell lysates were subjected to western blotting using p53, MDM2, p21, and Gapdh antibodies. Densitometric analysis showing the effect of miR-194 (white bars), miR-192 (gray bars), miR-215 (black bars) compared with Scr sequence (green bars) transfected cells of endogenous p53, MDM2, and p21 in MM1s ±SD (B) and NCI-H929 (C) Nutlin-3a treated. (D) Immunoblot analysis showing p53, MDM2, and p21 protein expression after 48 hr of miR-192, miR-194, miR-215 (pool), and Scr ASOs transfection in MM1s and NCI-H929 cells after 12 hr of treatment with 10 μM Nutlin-3a; Gapdh was internal loading control and densitometric analysis was reported ±SD (E). (F) MDM2 mRNA expression normalized for GAPDH mRNA expression in MM1s and NCI-H929 cells miRNAs or Scr transfected after Nutlin-3a treatment (6–12 hr) ±SD. (G) miRNAs predicted to interact with HDM2 gene in several consensus binding sites (XXX) at its 3′UTR, according to "in silico" RNA-22 prediction software. Luciferase assay showing decreased luciferase activity in cells cotransfected with pGL3-MDM2-3′UTR and miR-192, 194, 215, and Scr sequence. See also Figure S4. All experiments were performed in triplicate ±SD. (H) MDM2 mRNA relative expression in

3700 ± 950 mm^3 [$p < 0.01$]). The most effective combination was MI-219 plus miRs, where mice showed 5-fold reduced tumor volumes (from 5390 ± 993 mm^3 to 2100 ± 560 mm^3 [$p < 0.01$]) and >93% reduction when compared with VE/Scr treatment (Figure 5E). These findings demonstrate proof-of-concept for in vivo therapy of MM using combined miRNAs and an MDM2 pharmacological inhibitor.

miR-*192* and miR-*215*, by Antagonizing MDM2 Downregulation, Target IGF-1 and IGF1-R

Since our data demonstrate that miR-*192*, miR-*194*, and miR-*215* target *MDM2*, we sought to determine if MDM2 substrates could also be affected. IGF-1R is a known target of MDM2 ubiquitin ligase function (Girnita et al., 2003; Froment et al., 2008). Therefore, by targeting *MDM2*, miR-*192*, *194*, and *215* may indirectly influence the expression of IGF-1R. In MM cells, IGF-1R and its ligand, IGF-1, are key factors in regulation of PC migration into the bone marrow (Qiang et al., 2004; Tai et al., 2003). We noted that in WT *TP53* MM cells, p53 re-expression was strongly associated with downregulation of IGF-1R and IGF-1 (Figures S5A and S5B) compared with mutant *TP53* MM cells (Figures S5C and S5D). We sought to determine the effect of miRNAs on IGF-1R and IGF-1 expression through targeting MDM2. We found that in the presence of miR-*192*, *215* but not *miR-194*, IGF-1R and IGF-1 protein levels decreased, as determined by western blot analysis (Figure 6A). Furthermore, inhibition of endogenous miR-*192/215*, using antisense oligonucleotides, combined with 24 hr of Nutlin-3a treatments increased both IGF-1R and IGF-1 levels in MM1s cells (Figure 6B). This effect was not seen with miR-*194*. To determine if the regulation of IGF-1 does affect IGF1R in MM cells, we silenced IGF-1 and-observed upregulation of IGF-1R protein levels at 48 and 72 hr posttreatment (Figure 6C). This effect was clearly different from that observed following miRNA transfection (Figure 6A). We next tested whether miR-*192* and *215* target IGF-1R and IGF-1 directly by generating luciferase reporters containing their 3′ UTRs. Using Targetscan (Lewis et al., 2003), Pictar (Krek et al., 2005), and RNA22 (Miranda et al., 2006) searches, we identified several MREs for miR-*192* and miR-*215* but not for miR-*194* in the 3′UTR of *IGF-1R* and *IGF-1R* mRNAs (Figures 6D and 6E). Luciferase activity dropped 40%–50% when these constructs were cotransfected into MM1s cells with miR-*192*, *215* compared with miR-*194* and Scr (Figures 6D and 6E; Figures S5E–S5I). To determine if in freshly isolated CD-138+ PCs these miRNAs could regulate IGF-1 and IGF-1R expression, we transfected miR-*192* and *215* (pool) into PCs of nine patients, and we performed immunofluorescence analysis for IGF-1R and IGF-1 at 48 hr. We observed a significant decrease in IGF-1R and IGF-1 protein expression (Figures 6F and 6G). Transfection efficiency was confirmed using RNA Fluorescent Oligo (Figure 6H). These results indicate that miR-*192* and miR-*215* directly target *IGF-1R* and *IGF-1* in MM.

miR-*192* and *215* Block MM Migration and Invasion In Vitro and In Vivo

Given the known role of IGF-I and IGF-1R as antiapoptotic factors and in MM migration through endothelial barriers and bone marrow stroma (Qiang et al., 2004; Tai et al., 2003), we sought to determine if miR-*192* and *215* interfere with the chemotactic function of IGF-I and block migration and invasion of MM cells. We first determined that miR-*192* and *215* actions on the IGF-1 axis in MM affect both WT *TP53* (MM1s) and mutant (RPMI-8226) cell lines (Figure 7A) and that the downregulation of both proteins critically affects S6 and AKT phosphorylation in these cells. Next, we found that ectopic expression of miR-*192* and *215* in NCI-H929 and RPMI-8226 IGF-1-treated cells was associated with significant decrease in cell adhesion (Figures S6A and S6B), migration, and tissue invasion compared with Scr control. To this end, we used an intraepithelial trans-well migration assay with IGF-1 at various concentrations as attractant and two bone marrow-derived stromal cells, HS-5 (fibroblast-like) and HS-27A (epithelial-like) as cell layer. As shown in Figure 7B and Figure S6C, IGF-1 (50 ng/ml) stimulated migration of MM cells, MM1s, and RPMI-8226. To further examine the role of miRNA-*192, 215*, and *194* in MM cells, we investigated the effect of these miRNAs on migration in vivo, using a previously described homing model (Roccaro et al., 2009). Nine NOD-SCID mice (for each group) were intravenously injected with 8 × 10^6 of pre-miRNA-*192*-, *194*-, and *215*- or Scr probe-transfected GFP^+/Luc^+MM1S cells. One week later, mice were injected intravenously every week for 4 weeks with an individual miRNA or Scr dissolved in PBS (10 μg for each mouse). After 5 weeks, the homed and proliferated tumors were markedly suppressed in miRNA-treated mice compared with Scr-transfected MM cells ($p < 0.01$) (Figure 7C). At 5 weeks postinjection, we first noted reduced tumor progression, by bioluminescence imaging (Figure 7D). Mice injected with Scr-transfected MM1s in addition to serial intravenous injection with Scr showed significant tumor growth, but tumor burden was significantly reduced in mice injected with pre-miR-*194* and was nearly nonexistent in mice injected with either pre-miR*192* or pre-miR-*215* (Figures 7C and 7D). In addition, through FACS analysis using human CD-138+ antibody, we analyzed bone marrow engraftment of these cells in injected NOD-SCID mice. We confirmed that Scr-treated mice showed bone marrow engraftment of ~25% ± 15% of MM1s cells versus 4% ± 2% for miR-*192* and 2% ± 2% for miR-*215* animals (Figure 7E). The in vivo action of miR-*194* was less effective, 12% ± 3% of bone marrow engraftment MM1s cells compared with miR-*192* and *215* but still higher than the Scr control (Figure 7E). These data indicate that miR-*192*, *215* but also miR-*194* have therapeutic potential not only by affecting proliferation rates in MM cells but also by affecting the homing and migration ability of MM cells.

The Promoter Region of the miR-*194-2-192* Cluster is Hypermethylated in MM Cell Lines

During Nutlin-3a treatment of primary CD-138+ PCs from MMs without *TP53* deletion, we noted that p21 activation, as well as

CD138+ PCs from healthy, MGUS, and MM samples with determined by RT-PCR. Each data sample was normalized to the endogenous reference ACTIN by use of the 2– ct method. Kruskal-Wallis analysis assessed that MDM2 mRNA is differentially expressed among the healthy and MGUS samples vs MM PCs samples of the Bartlett test P value (<0.01) (see Table S3). (I) Graphic of the negative Spearman correlation coefficient ($\rho = -0.698$) corresponding to a decreasing monotonic trend between log of MDM2 mRNA relative expression and log of miR-192 relative expression ($p < 0.001$, $N = 33$).

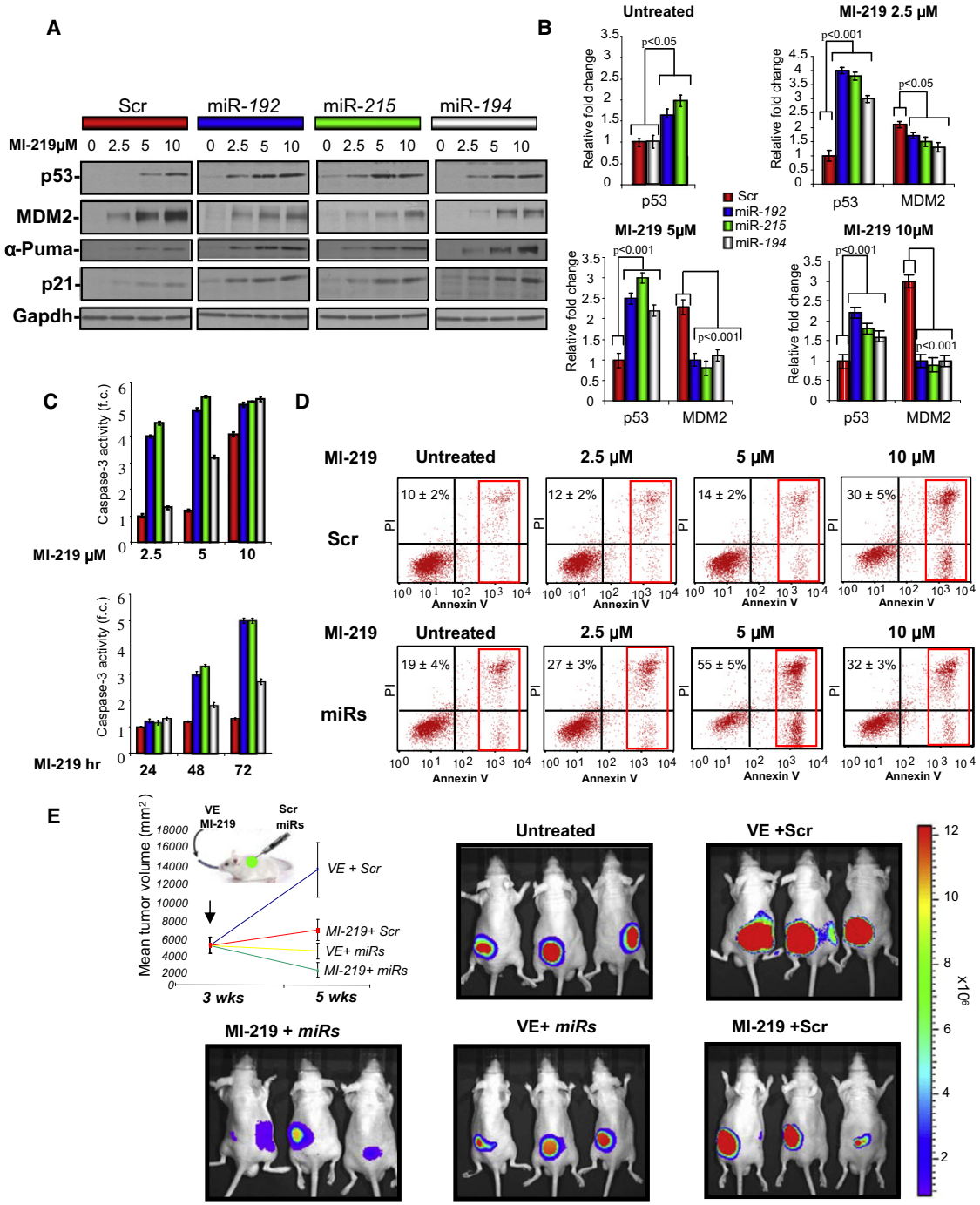

Figure 5. miR-*192*, *194*, and *215* Increase Sensitivity to MI-219 In Vitro and In Vivo by Targeting *MDM2*

(A) Effects of miR-192, 194 and 215 on endogenous p53, p21, and MDM2 levels (western blots) in MM1s cells treated with MI-219 at different concentrations. Densitometric analysis for p53 in untreated cells and for p53 and MDM2 protein levels in 2.5, 5, and 10 μM MI-219-treated cells is reported (B). All experiments were performed in triplicate ±SD.

(C) Apoptotic effect at different concentrations and time points for each miRNA-transfected cells was assessed by caspase-3 activation assay ±SD.

(D) Apoptosis associated with the pool of these miRNAs upon MI-219 treatment (24 hr) at different concentration (2.5–10 μM) was evaluated by Annexin V. All experiments were performed in triplicate ±SD.

(E) Gfp/Luc + MM1s cells were injected subcutaneously into the flanks of nude mice; at 3 weeks postinjection, mice with comparable tumor sizes were selected for treatment (untreated). In vivo confocal imaging of GFP+/Luc+ MM cells engrafted in athymic nu/nu mice after 2 weeks of combined treatment with oral MI-219 or vehicle (VE) plus pre-microRNA pool or Scr sequence directly into the tumors. Graphic represents the mean of tumors value (mm^2) before (3 weeks) and after the treatment (3+2 weeks) ±SD.

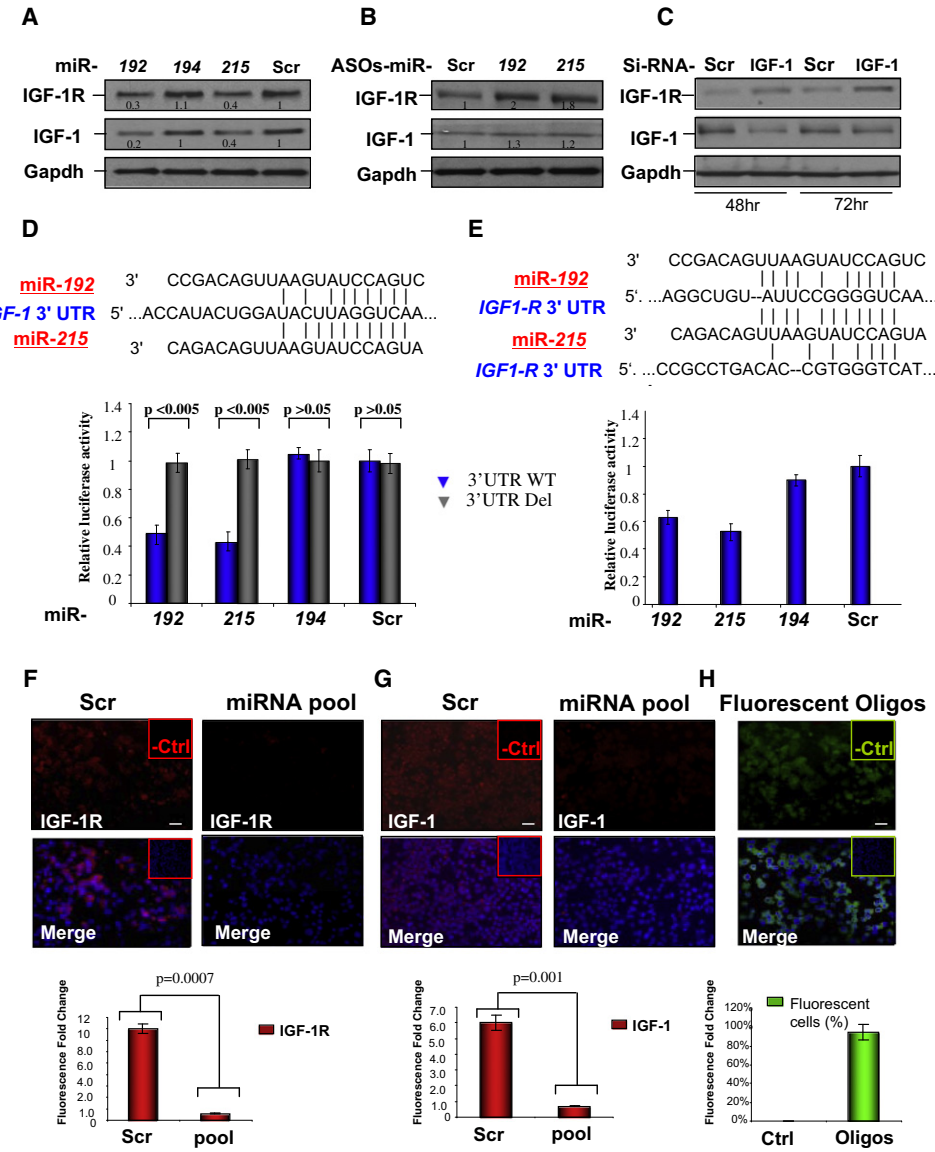

Figure 6. miR-*192-215* Regulate IGF-1 and IGF1-R Expression in MM Cells

(A and B) Western blot showing IGF-1R and IGF-1 expression after miR-*192* and miR-*215* transfection using pre (A) and ASOs (B) for miR-*192*, *215*, *194*, and Scr in MM1s cells treated for 12 hr with Nutlin-3a. Densitometric analysis is reported. See also Figure S5.

(C) Western blots after IGF-1 knockdown in MM1s (si-RNA) using anti-IGF-1R, IGF-1, and Gapdh antibodies.

(D and E) miRNAs predicted to interact with *IGF-1* and *IGF-1R* gene at their 3′UTR, according to "in silico" Target Scan (*IGF-1*) and RNA-22 (*IGF-1R*) prediction software (see also Figure S5). Luciferase assay showing decreased luciferase activity in MM1s cells cotransfected with pGL3-*IGF-1*-3′UTR (D) or pGL3-*IGF-1R*-3′UTR (full) (E) and miR-*192*, *194*, *215*, or Scr. Deletion of six bases in all putative consensus sequences on *IGF-1*-3′UTR abrogates these effect (Del) (D). See also Figure S5. Bars indicate relative luciferase activity ±SD. All experiments were performed in triplicate.

(F and G) Immunofluorescence using anti-IGF-1R (F) and anti-IGF-1 (G) in red and blue nuclear DNA, from CD-138+ PCs from nine MM patients transfected with miR-*192* and miR-*215* (pool) or Scr and intensity of the signal was assessed ±SD.

(H) The efficiency of the transfection in the nine samples was evaluated using fluorescent double-strand RNA oligos.

Scale bars indicate 25 μM.

re-expression of the three miRNAs, was consistent but not uniform in all samples analyzed. Possibly mechanisms other than alterations to the *TP53* gene could influence the sensitivity to MDM2 molecular inhibitors. In seeking an explanation for the lack of expression of these miRNAs in MMs, we noted that the genes for these miRNAs are located in chromosomal regions in MM that are normally characterized by chromosome gain and translocations rather than deletions (Fonseca et al., 2009). We then explored the methylation status in the promoter of the miR-*194-2-192* cluster. By combined bisulfite restriction analysis (COBRA), we detected hypermethylation of the promoter region of this cluster (Region R) (Figure S7A) in MM cell lines (Figure S7B). Furthermore, treatment of MM cell lines with a demethylation agent (Azacytidine) increased the expression

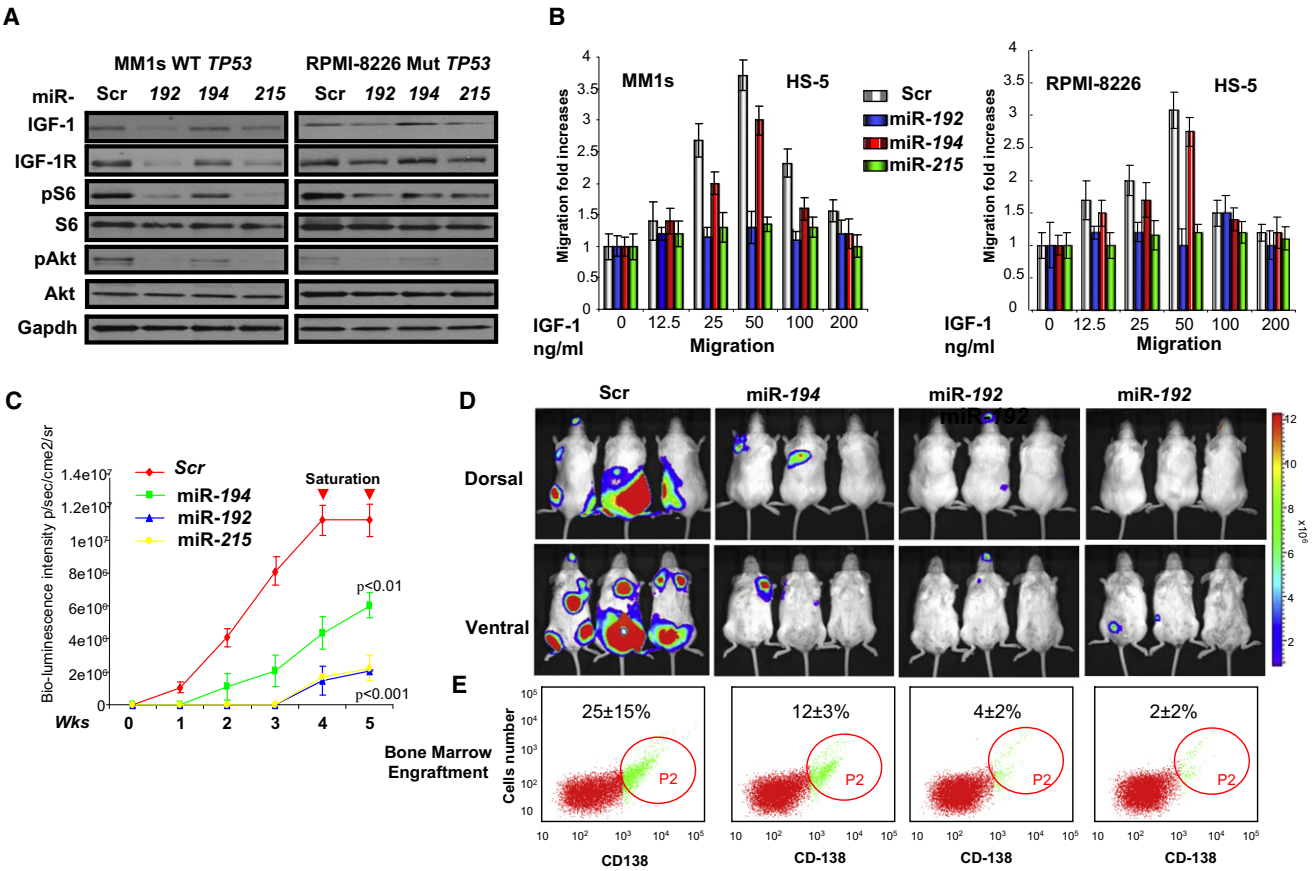

Figure 7. miR-*194*, *215*, and *194* Block Invasion Ability of MM Cells

(A) MM1s and RPMI-8226 cells (pre-miRNA-*192, 194, 215*, Scr-transfected) were harvested 72 hr after transfection. Whole-cell lysates were immunoblotted using IGF-1, IGF-1R, pS6, S6, p-Akt, Akt, and Gapdh antibodies; Scr sequence and miR-194-transfected cells served as controls. The experiments were performed in triplicate.

(B) Intraepithelial migration assay in MM cells miRNAs transfected using HS-5 cells at different concentrations of IGF-1 as attractant. Bars indicate relative fold change of migration compared with the control ±SD. See also Figure S6.

(C and D) In vivo confocal imaging. GFP+/Luc+ MM1s cells (8×10^6) were transfected using either pre-miRNA-*192, -194*, *215*, and Scr *RNA oligos* and then injected intravenously into mice immediately after transfection. After 1 week, the mice were injected intravenously with miRNAs (10 μg) once a week for 4 weeks, and the bioluminescence intensity was assessed before every injection (C). (D) Representative bioluminescence imaging (BLI) after 5 weeks from the injection.

(E) Bone marrow cells from the mice used for the experiment were isolated and human CD-138 positive cells (engrafted cells) were detected using anti-CD-138 antibody by flow cytometry (P2 fraction).

of these miRNAs in WT *TP53* MM cell lines (Figure S7C). Re-expression of the *SOCS-1* gene, known to be silenced by hypermethylation in MM cells (Galm et al., 2002), served as internal control.

DISCUSSION

Complex cytogenetic abnormalities and numeric chromosomal aberrations occur in virtually all multiple myeloma, and in most, if not all, cases of MGUS (Kuehl and Bergsagel, 2002). Paradoxically, mutations and/or deletion of *TP53* occur in only a small percentage of intramedullary MMs and not at all in MGUS (Chng et al., 2007). Several reports (Teoh et al., 1997; Quesnel et al., 1994) and our data (Figure 4E) suggest that MDM2 overexpression in MMs, but not its gene amplification (Quesnel et al., 1994), could be responsible for p53 inactivation in cells retaining functional p53 pathways. This supports the idea that induction of p53 in this setting might be a suitable treatment for MM. There have been a few reports concerning microRNA deregulation in MM and although not all reported findings were in agreement, they confirmed that such deregulation is important in MM pathogenesis (Pichiorri et al., 2008; Roccaro et al., 2009; Lionetti et al., 2009; Gutiérrez et al., 2010). Here, we studied the role of miRNAs in the p53 apoptotic pathway upon nongenotoxic activation of p53 in MM cells, using small molecular inhibitors of MDM2 (Nutlin-3a, MI-219). Upon p53 activation, we identified two related microRNA clusters located in regions considered important for MM (miR-*194-2-192* at 11q13.1 and miR-*194-1-215* at 1q41.1) (Fonseca et al., 2009). Furthermore, the knowledge that miRNAs coming from the same cluster can reinforce their action on the same cellular pathways (Garofalo et al., 2009; Ventura et al., 2008) led us to study the molecular mechanisms associated with activation of the p53 pathway by these miRNAs. Through characterization of the miR-*194-2-192* cluster

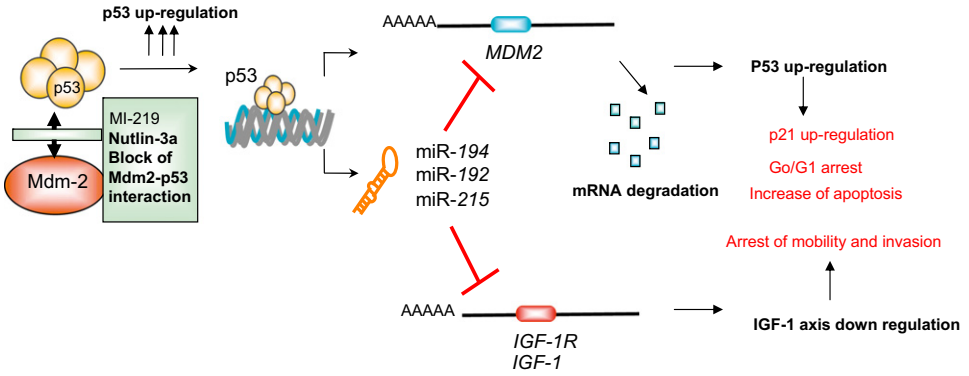

Figure 8. miR-*192*, *215*, and *194* Impair the p53/MDM2 Autoregulatory Loop
Model to illustrate the possible role of miR-*192, 194*, and *215* in control of MDM2 and IGF-1/IGF-1R pathways in MM cells. See also Figure S7.

promoter region and definition of a noncanonical p53 consensus site, we have shown that these miRNAs are direct p53 targets. In patient samples, the expression of these miRNAs changed during transition from normal PC, via MGUS to intramedullary MM; these miRNAs were significantly downregulated in a cohort of newly diagnosed MMs versus MGUS; miR-*192, 215*, and *194* enhanced colony suppression, cell-cycle arrest, or apoptosis in a p53-dependent manner. We also noted, as in the case of KMS28BM cells, that their biological action could be associated with the MDM2 status in MM cells. The short half-life of MDM2 protein (Marine et al., 2010) and difficulties in analyzing its protein expression in MM cells without p53 activation led to the demonstration that the effect of these miRNAs on MDM2 was clearly detectable after treating WT *TP53* MM cells with combined Nutlin-3a and ectopic expression of the miRNAs. In fact, we observed that in treated cells with enforced expression of these miRNAs MDM2 was dramatically downregulated at protein and mRNA levels and this downregulation was inversely associated with higher p53 expression and p21 activation (Figures 4A–4C). Luciferase assays using plasmids harboring the *MDM2* 3′UTR sequence strongly confirmed that *MDM2* is the direct target of these miRNAs. In a subset of newly diagnosed MMs, elevated levels of *MDM2* mRNA were inversely associated with miR-*192* expression. We proved, in vivo and in vitro, that the combination of these miRNAs with p53 pharmacological activator (MI-219), leading to MDM2 downregulation and subsequent p53, p21, and Puma upregulation, could be a successful therapeutic strategy. In fact, it produced anti-tumor results that could not be achieved solely by increasing the drug concentration. We also found that miR-*192* and miR-*215* expression, by overriding MDM2 ubiquitination of IGF-1R (Girnita et al., 2003; Froment et al., 2008), directly targets the IGF-1 axis in MM cells, controlling mobility and invasive properties of MM cells in vitro and in vivo. We propose a model in which these miRNAs are (1) regulators of the autoregulatory loop, increasing the window of time between p53 apoptotic action and p53 degradation by MDM2; and (2) at the same time targeting the IGF axis, antagonizing the MDM2 ubiquitin ligase function on IGF-1R (Figure 8).

The hypermethylation status in the promoter of the miR-*194-2-192* cluster in MM cell lines could support the hypothesis that the transition from MGUS to MM is favored by clonal selection of cells with aberrant promoter methylation of the miR-*194-2-192* cluster. This could be associated with a decreasing ability of p53 to downmodulate MDM2 expression thus tipping the regulatory balance in favor of MDM2 in MM cells. This proposed model (illustrated in Figure S7D) will require further investigation.

Of note, monoallelic deletion of *TP53* in MM, which often seems to occur without mutation on the other allele, is associated with an extremely poor prognosis (Chng et al., 2007). This supports the idea that a 2-fold decrease in *TP53* gene content is associated with tumor progression, which supports the hypothesis that a partial lack of expression of these miRNAs in MMs could create a p53 imbalance with direct biological consequences.

In summary, our results have defined a mechanism of p53 regulation through miRNAs acting on MDM2 expression, providing the basis for the development of miRNA-targeted therapies for MM, as illustrated in Figure 8.

EXPERIMENTAL PROCEDURES

Collection of Primary Cells

Thirty-three newly diagnosed primary MM samples, 14 primary samples from monoclonal gammopathy of undetermined significance (MGUS), and 5 primary samples from healthy donors were obtained from bone marrow aspirates. Written informed consent was obtained in keeping with institutional policies (IRB-approved procurement protocol (2000C0247) at Ohio State University and The University of Turin GIMEMA-MM-03-05, N. EUDRACT 2005-004745-33). Three of the five healthy PCs used were purchased from *AllCells* LLC (Emeryville, CA).

Luciferase Assays

MM1s cells were cotransfected with 1 μg of pGL3 firefly luciferase reporter vector (see luciferase reporter vector method in Supplemental Information), 0.1 μg of the phRL-SV40 control vector (Promega), and 100 nM miRNA precursors (Ambion) using nucleoporation (LONZA) Cell Line Nucleofector Kit V as previously described. Firefly and Renilla luciferase activities were measured consecutively by using the Dual Luciferase Assay (Promega) 24 hr after transfection. Each reporter plasmid was transfected at least twice (on different days) and each sample was assayed in triplicate.

Mouse Experiments

All animals were housed in the Ohio State University animal facility and the experiments with live animals were approved by our institute animal committee (IACUC 2007-A0146) and conducted following the Ohio State University animal policy in accordance with NIH guidelines.

GFP/Luc + MM1s cells (1×10^6) were suspended in 0.10 ml of extracellular matrix gel (BD Biosciences) and the mixture was injected subcutaneously into the right flank athymic nu/nu mice. Three weeks after injection, mice with comparable size tumors were treated for 2 weeks with a combination of oral dose of MI-219 (200 mg/kg) or vehicle, once a day for 14 days and miRNAs or scrambled sequence oligos (10 μg) (Ambion), was injected directly into the tumors once a week for 2 weeks. For the NOD-SCID engraftment model Luc+/GFP+ MM.1S cells (8×10^6/mouse) were injected into the tail vein of SCID mice. Treatment started 7 days from tumor cell inoculation, by weekly intravenous injections of miRNAs or scrambled sequence. RNA oligos (Ambion) (10 μg) for four cycles (4 weeks total). For more details, see in vivo experiments in Supplemental Information.

Transfection Method for Primary Cells and MM Cell Lines

CD-138+ PCs obtained from new diagnosed MM patients and isolated as previously described were transfected by using nucleoporation (LONZA) Cell Line Nucleofector Kit V (Cat#VCA-1003). MM1s, NCI-H929 cell lines were transfected by using nucleoporation (LONZA) Cell Line Nucleofector Kit V (Cat#VCA-1003). Instead for U266, KMS-28BM, and RPMI-8226, Cell Line Nucleofector Kit C (Cat#VCA-1004) was used. Specifically for primary cells 1×10^6 CD-138+ PCs were resuspended in 100 μl V solution and 100 nM miRNA precursors (Ambion) was used for the transfection reaction. For more details, see transfection method for primary cells in Supplemental Information.

Target Screening

In this study, we used three publicly available search engines for target prediction to obtain the putative targets: TargetScan (Release 2.1), http://genes.mit.edu/targetscan, Pictar, http://pictar.bio.nyu.edu, and Rna22, http://cbcsrv.watson.ibm.com/rna22_targets.html. For RNA22 predicted sites, we considered only the heteroduplex with a folding energy > −27 Kcal/mol (Figures S8B–S8E) because we were not able to confirm by luciferase assay the interactions between target gene and miRNAs with a folding energy less that −27 Kcal/mol (data not shown).

ACCESSION NUMBERS

The microarray data have been deposited in the Array Express database, www.ebi.ac.uk/arrayexpress (accession number E-TABM-1037 and E-TABM-1038).

SUPPLEMENTAL INFORMATION

Supplemental Information includes Experimental Procedures, references, seven figures, and three tables and can be found online at doi:10.1016/j.ccr.2010.09.005.

ACKNOWLEDGMENTS

We thank Kay Huebner for careful reading of the draft MS, Nicola Zanesi for helping with the animal procedures, Dorothee Wernicke for helpful scientific discussion, Michele Morara for statistical advice, Yuri Pekarsky for scientific advice, Guido Marcucci and Ramiro Garzon for scientific advice, and Sharon Palko for administrative support. We also thank Dr. Shaomeng Wang's laboratory for supplying MI-219 compound and Dr. Irene M. Ghobrial for providing MM1s GFP+/Luc+ cells. We are grateful for research support from the Ohio State University Targeted Investment in Excellence Award and the Kimmel Foundation award (F.P.).

Received: April 19, 2010
Revised: June 16, 2010
Accepted: August 9, 2010
Published: October 18, 2010

REFERENCES

Bartel, D.P. (2004). MicroRNAs: genomics, biogenesis, mechanism, and function. Cell *116*, 281–297.

Braun, C.J., Zhang, X., Savelyeva, I., Wolff, S., Moll, U.M., Schepeler, T., Ørntoft, T.F., Andersen, C.L., and Dobbelstein, M. (2008). p53-Responsive microRNAs 192 and 215 are capable of inducing cell cycle arrest. Cancer Res. *68*, 10094–10104.

Chang, T.C., Yu, D., Lee, Y.S., Wentzel, E.A., Arking, D.E., West, K.M., Dang, C.V., Thomas-Tikhonenko, A., and Mendell, J.T. (2008). Widespread microRNA repression by Myc contributes to tumorigenesis. Nat. Genet. *40*, 43–50.

Chng, W.J., Glebov, O., Bergsagel, P.L., and Kuehl, W.M. (2007). Genetic events in the pathogenesis of multiple myeloma. Best Pract. Res. Clin. Haematol. *20*, 571–596.

Croce, C.M. (2008). Oncogenes and cancer. N. Engl. J. Med. *358*, 502–511.

Danovi, D., Meulmeester, E., Pasini, D., Migliorini, D., Capra, M., Frenk, R., De Graaf, P., Francoz, S., Gasparini, P., Gobbi, A., et al. (2004). Amplification of Mdmx (or Mdm4) directly contributes to tumor formation by inhibiting p53 tumor suppressor activity. Mol. Cell Biol. *24*, 5835–5843.

Dickens, M.P., Fitzgerald, R., and Fischer, P.M. (2009). Small-molecule inhibitors of MDM2 as new anticancer therapeutics. Semin. Cancer Biol. *20*, 10–18.

Fonseca, R., Bergsagel, P.L., Drach, J., Shaughnessy, J., Gutierrez, N., Stewart, A.K., Morgan, G., Van Ness, B., Chesi, M., Minvielle, S., et al. (2009). International Myeloma Working Group molecular classification of multiple myeloma: spotlight review. Leukemia *23*, 2210–2221.

Froment, P., Dupont, J., and Christophe-Marine, J. (2008). Mdm2 exerts pro-apoptotic activities by antagonizing insulin-like growth factor-I-mediated survival. Cell Cycle *7*, 3098–3103.

Galm, O., Yoshikawa, H., Esteller, M., Osieka, R., and Herman, J.G. (2002). SOCS-1, a negative regulator of cytokine signaling, is frequently silenced by methylation in multiple myeloma. Blood *101*, 2784–2788.

Garofalo, M., Di Leva, G., Romano, G., Nuovo, G., Suh, S.S., Ngankeu, A., Taccioli, C., Pichiorri, F., Alder, H., Secchiero, P., et al. (2009). miR-221&222 regulate TRAIL resistance and enhance tumorigenicity through PTEN and TIMP3 downregulation. Cancer Cell *16*, 498–509.

Georges, S.A., Biery, M.C., Kim, S.Y., Schelter, J.M., Guo, J., Chang, A.N., Jackson, A.L., Carleton, M.O., Linsley, P.S., Cleary, M.A., et al. (2008). Coordinated regulation of cell cycle transcripts by p53-inducible microRNAs, miR-192 and miR-215. Cancer Res. *68*, 10105–10112.

Girnita, L., Girnita, A., and Larsson, O. (2003). Mdm2-dependent ubiquitination and degradation of the insulin-like growth factor 1 receptor. Proc. Natl. Acad. Sci. USA *100*, 8247–8252.

Gutiérrez, N.C., Sarasquete, M.E., Misiewicz-Krzeminska, I., Delgado, M., De Las Rivas, J., Ticona, F.V., Fermiñán, E., Martín-Jiménez, P., Chillón, C., Risueño, A., et al. (2010). Deregulation of microRNA expression in the different genetic subtypes of multiple myeloma and correlation with gene expression profiling. Leukemia *24*, 629–637.

He, L., He, X., Lowe, S.W., and Hannon, G.J. (2007). microRNAs join the p53 network—another piece in the tumour-suppression puzzle. Nat. Rev. Cancer *7*, 819–822.

Hermeking, H. (2010). The miR-34 family in cancer and apoptosis. Cell Death Differ. *17*, 193–199.

Hino, K., Tsuchiya, K., Fukao, T., Kiga, K., Okamoto, R., Kanai, T., and Watanabe, M. (2008). Inducible expression of microRNA-194 is regulated by HNF-1alpha during intestinal epithelial cell differentiation. RNA *14*, 1433–1442.

Junttila, M.R., and Evan, G.I. (2009). p53—a Jack of all trades but master of none. Nat. Rev. Cancer *9*, 821–829.

Krek, A., Grün, D., Poy, M.N., Wolf, R., Rosenberg, L., Epstein, E.J., MacMenamin, P., da Piedade, I., Gunsalus, K.C., Stoffel, M., et al. (2005). Combinatorial microRNA target prediction. Nat. Genet. *37*, 495–500.

Kuehl, W.M., and Bergsagel, P.L. (2002). Multiple myeloma: evolving genetic events and host interactions. Nat. Rev. Cancer *2*, 175–187.

Lane, D. (2001). How cells choose to die. Nature *414*, 25–27.

Lewis, B.P., Shih, I., Jones-Rhoades, M., Bartel, D., and Burge, C. (2003). Prediction of mammalian microRNA targets. Cell *115*, 787–798.

Lionetti, M., Biasiolo, M., Agnelli, L., Todoerti, K., Mosca, L., Fabris, S., Sales, G., Deliliers, G.L., Bicciato, S., Lombardi, L., et al. (2009). Identification of

microRNA expression patterns and definition of a microRNA/mRNA regulatory network in distinct molecular groups of multiple myeloma. Blood *114*, 20–26.

Marine, J.C., and Lozano, G. (2010). Mdm2-mediated ubiquitylation: p53 and beyond. Cell Death Differ. *17*, 93–102.

Miranda, K.C., Huynh, T., Tay, Y., Ang, Y.S., Tam, W.L., Thomson, A.M., Lim, B., and Rigoutsos, I. (2006). A pattern-based method for the identification of microRNA binding sites and their corresponding heteroduplexes. Cell *126*, 1203–1217.

Park, S.Y., Lee, J.H., Ha, M., Nam, J.W., and Kim, V.N. (2009). miR-29 miRNAs activate p53 by targeting p85 alpha and CDC42. Nat. Struct. Mol. Biol. *16*, 23–29.

Ooi, M.G., Hayden, P.J., Kotoula, V., McMillin, D.W., Charalambous, E., Daskalaki, E., Raje, N.S., Munshi, N.C., Chauhan, D., Hideshima, T., et al. (2009). Interactions of the Hdm2/p53 and proteasome pathways may enhance the antitumor activity of bortezomib. Clin. Cancer Res. *15*, 7153–7160.

Pichiorri, F., Suh, S.S., Ladetto, M., Kuehl, M., Palumbo, T., Drandi, D., Taccioli, C., Zanesi, N., Alder, H., Hagan, J.P., et al. (2008). MicroRNAs regulate critical genes associated with multiple myeloma pathogenesis. Proc. Natl. Acad. Sci. USA. *105*, 12885–12890.

Qiang, Y.W., Yao, L., Tosato, G., and Rudikoff, S. (2004). Insulin-like growth factor I induces migration and invasion of human multiple myeloma cells. Blood *103*, 301–308.

Quesnel, B., Preudhomme, C., Oscier, D., Lepelley, P., Collyn-d'Hooghe, M., Facon, T., Zandecki, M., and Fenaux, P. (1994). Over-expression of the MDM2 gene is found in some cases of haematological malignancies. Br. J. Haematol. *88*, 415–418.

Roccaro, A.M., Sacco, A., Thompson, B., Leleu, X., Azab, A.K., Azab, F., Runnels, J., Jia, X., Ngo, H.T., Melhem, M.R., et al. (2009). MicroRNAs 15a and 16 regulate tumor proliferation in multiple myeloma. Blood. *113*, 6669–6680.

Saha, M.N., and Chang, H. (2010). Pharmacological activation of the p53 pathway in haematological malignancies. J. Clin. Pathol. *63*, 204–209.

Shangary, S., Qin, D., McEachern, D., Liu, M., and Miller, R.S. (2008). Temporal activation of p53 by a specific MDM2 inhibitor is selectively toxic to tumors and leads to complete tumor growth inhibition. Proc. Natl. Acad. Sci. USA *105*, 3933–3938.

Sinha, A.U., Kaimal, V., Chen, J., and Jegga, A.G. (2008). Dissecting microregulation of a master regulatory network. BMC Genomics *23*, 88.

Song, B., Wang, Y., Kudo, K., Gavin, E.J., Xi, Y., and Ju, J. (2008). miR-192 Regulates dihydrofolate reductase and cellular proliferation through the p53-microRNA circuit. Clin. Cancer Res. *14*, 8080–8086.

Stuhmer, T., and Bargou, R.C. (2006). Selective pharmacologic activation of the p53-dependent pathway as a therapeutic strategy for hematologic malignancies. Cell Cycle *5*, 39–42.

Tai, Y.T., Podar, K., Catley, L., Tseng, Y.H., Akiyama, M., Shringarpure, R., Burger, R., Hideshima, T., Chauhan, D., Mitsiades, N., et al. (2003). Insulin-like growth factor-1 induces adhesion and migration in human multiple myeloma cells via activation of beta1-integrin and phosphatidylinositol 3′-kinase/AKT signaling. Cancer Res. *63*, 5850–5858.

Teoh, G., Urashima, M., Ogata, A., Chauhan, D., DeCaprio, J.A., Treon, S.P., Schlossman, R.L., and Anderson, K.C. (1997). MDM2 protein overexpression promotes proliferation and survival of multiple myeloma cells. Blood *90*, 1982–1992.

Weiss, B.M., Abadie, J., Verma, P., Howard, R.S., and Kuehl, W.M. (2009). A monoclonal gammopathy precedes multiple myeloma in most patients. Blood *113*, 5418–5422.

Ventura, A., Kirsch, D.G., McLaughlin, M.E., Tuveson, D.A., Grimm, J., Lintault, L., Newman, J., Reczek, E.E., Weissleder, R., and Jacks, T. (2007). Restoration of p53 function leads to tumour regression in vivo. Nature *445*, 661–665.

Ventura, A., Young, A.G., Winslow, M.M., Lintault, L., Meissner, A., Erkeland, S.J., Newman, J., Bronson, R.T., Crowley, D., Stone, J.R., et al. (2008). Targeted deletion reveals essential and overlapping functions of the miR-17 through 92 family of miRNA clusters. Cell *132*, 875–886.

Xue, W., Zender, L., Miething, C., Dickins, R.A., Hernando, E., Krizhanovsky, V., Cordon-Cardo, C., and Lowe, S.W. (2007). Senescence and tumour clearance is triggered by p53 restoration in murine liver carcinomas. Nature *445*, 656–660.

Zhang, Y., Gao, J.S., Tang, X., Tucker, L.D., Quesenberry, P., Rigoutsos, I., and Ramratnam, B. (2009). MicroRNA 125a and its regulation of the p53 tumor suppressor gene. FEBS Lett. *583*, 3725–3730.